values of clear water L_W^λ measured at other times for approximately the same solar elevation. When this is done for station 10, with an area south of Key West used as representative of clear water, the resulting derived pigment concentrations from R_1 and R_2 are, respectively, 0.21 and 0.33 mg m^{-3}. If the values of L_W^λ measured aboard the R.V. *Athena II* at station 10 are used to estimate $\alpha(\lambda, 670)$, the derived concentrations are 0.33 and 0.26 mg m^{-3}, respectively. The measured pigment concentration at station 10 was 0.36 mg m^{-3}. Clearly, this technique shows considerable promise for estimating pigment concentrations in regions where surface measurements are not available.

The limited results presented here suggest that maps of phytoplankton pigment concentration can presently be derived from CZCS imagery to better than 0.5 log C. Furthermore, the corrected CZCS imagery reveals circulation patterns heretofore unobserved in satellite imagery of the Gulf of Mexico. A CZCS-type system can be of considerable value in augmenting the study of complex coastal circulation processes and ecology.

HOWARD R. GORDON
Department of Physics,
University of Miami,
Coral Gables, Florida 33124
DENNIS K. CLARK
National Environmental Satellite Service, National Oceanic and Atmospheric Administration, Washington, D.C. 20233
JAMES L. MUELLER
Laboratory for Atmospheric Sciences, National Aeronautics and Space Administration, Goddard Space Flight Center, Greenbelt, Maryland 20771
WARREN A. HOVIS
National Environmental Satellite Service, National Oceanic and Atmospheric Administration

References and Notes

1. W. A. Hovis *et al.*, *Science* **210**, 60 (1980).
2. A. Morel and L. Prieur, *Limnol. Oceanogr.* **22**, 709 (1977).
3. In addition to the absorption effects of Chl *a* and Phaeo *a*, the accessory pigments chlorophyll *c* and carotenoids also contribute to the total absorbance within the 443-nm band. These effects are assumed to covary with *C*.
4. H. R. Gordon and D. K. Clark, *Boundary-Layer Meteorol.*, in press.
5. W. A. Hovis and K. C. Leung, *Opt. Eng.* **16**, 157 (1977).
6. G. L. Clarke, G. C. Ewing, C. J. Lorenzen, *Science* **167**, 1119 (1970); J. C. Arvesen, J. P. Millard, E. C. Weaver, *Astronaut. Acta* **18**, 229 (1973).
7. C. S. Yentsch and D. W. Menzel, *Deep-Sea Res.* **10**, 221 (1963); O. Holm-Hansen, C. J. Lorenzen, R. W. Holmes, J. D. H. Strickland, *J. Cons. Cons. Perm. Int. Explor. Mer* **30**, 3 (1965).
8. H. R. Gordon, *Appl. Opt.* **17**, 1631 (1978).
9. ———, *ibid.* **15**, 1974 (1976).
10. Specifically, $\alpha(\lambda_1,\lambda_2)$ is equal to the product of the ratios of the aerosol optical thicknesses, the single scattering albedos, and the extraterrestrial solar irradiances (after accounting for ozone absorption) at the two wavelengths in question.
11. The ship track and station 10 location are probably navigated to no better than 12 pixels with respect to the imagery. A more accurate location for station 10 could result in a more accurate atmospheric correction.
12. We acknowledge the assistance of D. Ball of Computer Sciences Corporation in the production of the results and figures presented in this report. We also thank Dr. A. E. Strong, Dr. E. T. Baker, H. Stumpf, R. Comeyne, E. King, J. Kapsch, R. Hill, and S. Roman of the National Oceanic and Atmospheric Administration; Dr. D. Kiefer and J. SooHoo of the University of Southern California; Dr. W. Broenkow of San Jose State University; and the captain and crew of the R.V. *Athena II* for their indispensable assistance in the collection of the in situ oceanographic data. One of us (H.R.G.) was supported by NASA contract NAS 5-22963.

7 November 1979; revised 31 March 1980

Atmospheric Carbon Dioxide, the Southern Oscillation, and the Weak 1975 El Niño

Abstract. *The observed rate of change of the atmospheric carbon dioxide concentration at the South Pole, Fanning Island, Hawaii, and ocean weather station P correlates with an index of the southern oscillation and with El Niño occurrences. There are changes at all four stations that seem to be in response to the weak 1975 El Niño. Thus, even poorly developed El Niño events may affect the atmospheric carbon dioxide concentration.*

The rate of change of the atmospheric concentration of CO_2 at the South Pole and at Mauna Loa, Hawaii, has been shown to be significantly correlated with a southern oscillation index (SOI) (*1*). The southern oscillation is a large-scale atmospheric and hydrospheric fluctuation centered in the equatorial Pacific Ocean and involving wind strengths, ocean currents, and sea-surface temperatures (*2*). It has a variable period, averaging approximately 4 years. El Niño occurrences are probably the most spectacular of the phenomena associated with the southern oscillation. Changes in atmospheric CO_2 have been observed that correspond to the El Niño's of 1965, 1969, and 1972 (*3*).

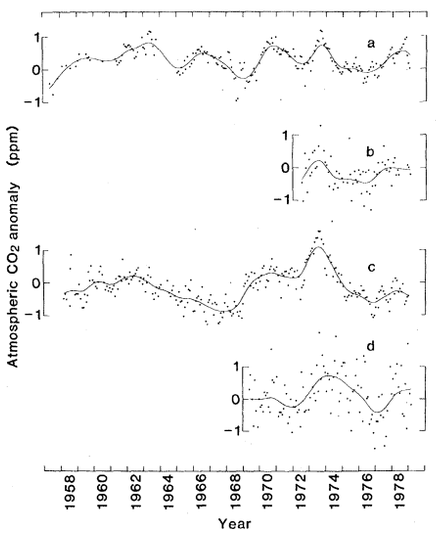

Fig. 1. Atmospheric CO_2 anomalies at (a) the South Pole, (b) Fanning Island (4°N), (c) Mauna Loa, Hawaii (20°N), and (d) Canadian ocean weather station P (50°N). The anomaly curves are spline fits to data from which an average seasonal effect and a smooth trend have been removed.

Correlations between SOI and the rate of change of atmospheric CO_2 at Fanning Island, near the equator (4°N), and at ocean weather station P, off the Canadian west coast (50°N), as reported here, tend to confirm the association. There are changes at all four stations that correspond to the 1972 and 1976 El Niño events, and, seemingly, to the weak 1975 El Niño as well.

The El Niño of 1975 was so weak that it probably would not have been recognized as an El Niño, were it not so well studied (*4*, *5*). El Niño refers to an oceanic and meteorological disturbance in the Peruvian coastal area apparently caused by an invasion of warm, nutrient-poor surface water into an area normally occupied by colder, more nutrient-rich water of upwelling origin. A fully developed El Niño is characterized by torrential rains in the normally arid coastal region and disruption of the large anchovy fishery as the fish seek colder, more nutrient-rich water.

The prediction of the 1975 El Niño by Quinn (*6*) led to the El Niño Watch Expedition, which systematically collected oceanographic data in the region west of the South American coast, from 5°N to 15°S. In February and March 1975, a thin tongue (10 to 25 m thick) of low-salinity, warm, nutrient-poor water extended south across the equator eastward of the Galápagos Islands, but the Peruvian coastal region and its fishery were essentially undisturbed. The invasion of warm surface water was short-lived; by May, conditions had returned to near normal. Wyrtki *et al.* (*4*) have suggested that the term El Niño be reserved for the spec-

0036-8075/80/1003-0066$00.50/0

tacular events lasting a year or more, but here we follow the usage of others (*5*) and refer to an undeveloped El Niño as a weak El Niño.

The occurrence of El Niño is an integral part of the southern oscillation (*7*). A suitable SOI is the pressure difference between Easter Island and Darwin, Australia, smoothed by a 12-month running mean (*8*). Fully developed El Niño events, such as occurred in 1965, 1969, 1972, and 1976, are observed to coincide with a minimum of SOI and usually start soon after the beginning of a year. The results of the El Niño Watch Expedition support the hypothesis that all minima of SOI are accompanied by El Niño-type conditions, even if a fully developed El Niño does not occur.

The effect of the southern oscillation on the atmospheric CO_2 concentration can be seen in the "anomaly" curves of Fig. 1, and more clearly in Fig. 2, where inverted time derivatives of the anomaly curves are shown together with a plot of the SOI. The anomaly curves are spline fits to atmospheric CO_2 data from which have been removed both an average seasonal effect and an approximately exponential trend (*9*), which represents the effect of fossil fuel combustion.

The rate of change of the CO_2 anomaly rather than the anomaly itself would be expected to correlate more closely with an atmospheric and hydrospheric phenomenon such as the southern oscillation (*1*), and indeed this is the case (Table 1). The correlation is such that low SOI corresponds to rising atmospheric CO_2 concentration, as would be produced by a net transfer of CO_2 from the oceans to the atmosphere. High SOI corresponds to falling CO_2 concentration.

The lags in the correlation are suggestive of a phenomenon driven by the equatorial region (*3*). The lag in the rate of change of the CO_2 concentration relative to SOI is 1 month at Fanning Island (4°N), 3 months at Mauna Loa (20°N), 7 months at station P (50°N), and 6 months at the South Pole.

It is rather surprising that all the curves in Fig. 2 seem to show a response to the weak 1975 El Niño. The responses are very small, especially at station P, and probably would not be credible except that they all line up approximately with the 1975 SOI minimum.

The mechanism that connects the southern oscillation and the CO_2 concentration is not entirely clear. Equatorial sea-surface temperature change is the leading explanation (*3, 10, 11*), but other explanations are possible (*1*). High SOI is accompanied by intensified circulation of the South Pacific gyre. The trade winds, the equatorial currents, and upwelling along the west coast of South America and the equator are all increased. The equatorial countercurrents are weakened. Sea-surface temperature is lower than average in the upwelling regions. Low SOI brings weakened trade winds, weakened or no upwelling, and warmer sea-surface temperatures in the upwelling regions.

Table 1. Correlation coefficients between the inverted anomaly derivatives, the inverted anomalies, and the southern oscillation index (SOI). The lags are with respect to SOI. The two closest peaks to zero lag are given. The indicated errors are an estimate of the standard deviation at zero lag if the time series were uncorrelated (*17*).

Inverted anomaly derivative		Inverted anomaly	
Correlation coefficient	Lag (months)	Correlation coefficient	Lag (months)
	South Pole (90°S)		
.69 ± .29	6	−.49 ± .27	−4
−.44 ± .29	−14	.43 ± .27	17
	Fanning Island (4°N)		
.80 ± .37	1	−.48 ± .46	−8
−.15 ± .37	−12	.78 ± .46	11
	Mauna Loa (20°N)		
.52 ± .25	3	−.43 ± .21	−7
−.49 ± .25	−27	.09 ± .21	14
	Station P (50°N)		
.66 ± .36	7	−.57 ± .34	−4
−.57 ± .36	−16	.33 ± .34	19

The region where the sea-surface temperature is most strongly affected by the southern oscillation has been identified by Weare *et al.* (*12*) through an empirical orthogonal analysis of Pacific Ocean sea-surface temperature. As might be expected, this region is the upwelling area along the equator and the west coast of South America (*13*).

For the sea-surface temperature change explanation to be valid, the surface layer of the ocean must be capable

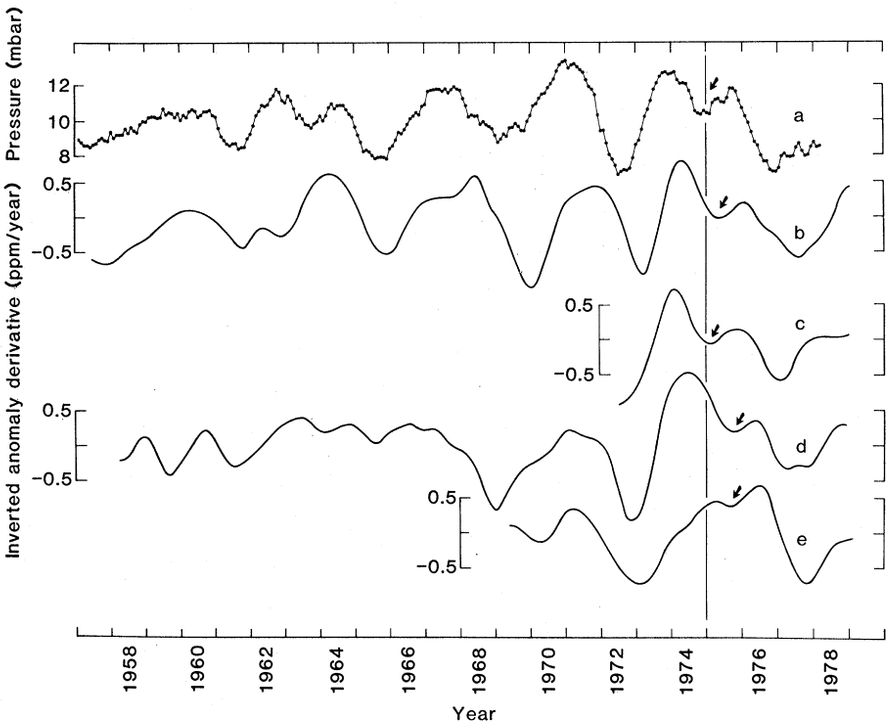

Fig. 2. Southern oscillation index (SOI) (a) and inverted time derivatives of the anomaly curves in Fig. 1 at (b) the South Pole, (c) Fanning Island, (d) Mauna Loa, and (e) station P. Fully developed El Niño events occurred in 1965, 1969, 1972, and 1976, and a weak El Niño occurred in 1975. The SOI minimum corresponding to the weak 1975 El Niño and the apparent responses are indicated by arrows.

of supplying the observed increase in atmospheric CO_2, when the ocean surface is warmed by an amount typical of the southern oscillation (El Niño) cycle. A simple equilibrium model calculation (*14*) predicts about one-half the observed amplitude, which is probably sufficiently close agreement.

The problem with the sea-surface temperature explanation of the atmospheric CO_2 response to the southern oscillation is that upwelled water is rich in CO_2. The equatorial upwelling region appears to be a large and persistent source of CO_2 to the atmosphere. Measurements of the partial pressure of CO_2 exerted by surface sea-water (pCO_2) in the upwelling region are above the atmospheric CO_2 partial pressure by as much as 80 parts per million (ppm) (*15*), presumably because of the recent upwelling of the surface water. Reduced upwelling might be expected to reduce the atmospheric CO_2 concentration, exactly opposite to the observations.

If equatorial sea-surface temperature change is the cause of the connection between the southern oscillation and atmospheric CO_2 concentration, then pCO_2 must be lower in the colder but presumably CO_2-richer water at an SOI maximum than during an SOI minimum. This could probably be accounted for if vertical water exchange and thermal balance were introduced into the model, in addition to CO_2 balance.

Biotic processes may also be important (*16*). Recently upwelled water is rich in the nutrients nitrogen and phosphorus, in addition to CO_2. A plankton bloom in response to these nutrients would be expected to reduce pCO_2 at an SOI maximum.

The hypothesis that pCO_2 is lower in Pacific equatorial water during an SOI maximum than during an SOI minimum should be tested. A time series of pCO_2 measurements in the Pacific equatorial upwelling region could be obtained during an El Niño cycle. The El Niño need not be fully developed; a study conducted during one as weak as the 1975 El Niño would do much to resolve the question of the mechanism by which the southern oscillation influences atmospheric CO_2.

R. B. BACASTOW, J. A. ADAMS*
C. D. KEELING, D. J. MOSS
T. P. WHORF
Scripps Institution of Oceanography, University of California, San Diego, La Jolla 92093
C. S. WONG
Marine Carbon Research Centre, Canadian Institute of Ocean Sciences, Sidney, British Columbia V8L 482

References and Notes

1. R. Bacastow, *Nature (London)* **261**, 116 (1976).
2. H. P. Berlage, *Meded. Verh. K. Ned. Meteorol. Inst.* **88**, 19 (1966).
3. L. Machta, K. Hanson, C. D. Keeling, in *The Fate of Fossil Fuel CO_2 in the Oceans*, N. R. Andersen and A. Malahoff, Eds. (Plenum, New York, 1977), p. 131.
4. K. Wyrtki, E. Stroup, W. Patzert, R. Williams, W. Quinn, *Science* **191**, 343 (1976).
5. T. J. Cowles, R. T. Barber, O. Guillen, *ibid.* **195**, 285 (1977).
6. W. H. Quinn, *Coastal Upwelling Ecosyst. Anal. Newsl.* **3**, 12 (1974).
7. ———, *J. Appl. Meteorol.* **13**, 825 (1974).
8. ——— and W. V. Burt, *ibid.* **11**, 616 (1972).
9. R. Bacastow, in *The Fate of Fossil Fuel CO_2 in the Oceans*, N. R. Andersen and A. Malahoff, Eds. (Plenum, New York, 1977), p. 33.
10. R. E. Newell and B. C. Weare, *Geophys. Res. Lett.* **4**, 1 (1977); F. MacIntyre, *Climatic Change* **1**, 349 (1978).
11. R. Bacastow, *J. Geophys. Res.* **84**, 3108 (1979).
12. B. C. Weare, A. R. Navato, R. E. Newell, *J. Phys. Oceanogr.* **6**, 671 (1976).
13. The correlation coefficient between the time coefficients of NS1, the empirical orthogonal function that represents the largest part of the variance of the Pacific Ocean nonseasonal temperature field north of −20°S [extended through 1976 (R. E. Newell and A. R. Navato, personal communication)] and SOI is −.76 ± .18 and the lag of NS1 is approximately 1 month. This result is consistent with the idea that sea-surface temperature changes associated with the southern oscillation are in response to changes in upwelling rate caused by changes in wind strength, since SOI is closely related to trade wind strength.
14. The size of this region [as indicated by the area where the NS1 of Weare *et al.* (*12*) is large] is approximately 18 × 10^6 km^2, about 1/20th of the area of the world's oceans. The change in sea-surface temperature associated with the southern oscillation is about 5°C [(*12*); R. E. Newell, personal communication]. A model consisting of a surface ocean layer with an area 1/20th that of the oceans and a depth of 100 m, in equilibrium with the entire atmosphere, would lead to the prediction that a temperature change of 5°C would correspond to an atmospheric CO_2 change of 0.4 part per million [equation 8 in (*11*)]. The observed total anomaly amplitude is about 1 part per million.
15. C. D. Keeling, N. W. Rakestraw, L. S. Waterman, *J. Geophys. Res.* **70**, 6087 (1965); Y. Miyake, Y. Sugimura, K. Saruhashi, *Rec. Oceanogr. Works Jpn.* **12**, 45 (1974).
16. R. E. Newell, A. R. Navato, J. Hsiung, *Pure Appl. Geophys.* **116**, 351 (1978).
17. G. E. P. Box and G. M. Jenkins, *Time Series Analysis* (Holden-Day, San Francisco, 1970).
18. This work was supported by the Climate Dynamics Program of the National Science Foundation (grant ATM 77-25141), with funds provided by the National Science Foundation, the National Oceanic and Atmospheric Administration, and the Department of Energy.
* Present address: Sperry-Univac Corporation, 4455 Morena Boulevard, San Diego, Calif. 92117.

30 July 1979; revised 10 June 1980

Geochronology of Wadi Tushka: Lost Tributary of the Nile

Abstract. *The Sadat Canal, now under construction, is designed to drain excess water from Lake Nasser to the Western Desert by way of Wadi Tushka, a sand-filled, dry-wash tributary of the Nile 34 kilometers north of Abu Simbel. Core-drilling logs made by the Aswan High Dam Authority prior to excavation of the Sadat Canal and along 48 kilometers of its axis reveal as much as 33 meters of unconsolidated sand and gravel over Mesozoic bedrock and under surficial dune sand and playa muds of Holocene age. Excavation of the canal revealed Acheulean artifacts 6.7 meters below the surface in fluvial sediments capped by a buried, red calcic paleosol. These data are interpreted as evidence for the existence of a major tributary of the Nile during the late middle Pleistocene. The tributary drained the Kiseiba-Dungul Depression and possibly the Kharga Depression as well. Chalcedony-armored mudstones in the depressions are believed to be saline lake deposits possibly related to a lake that drained to the Nile by way of Wadi Tushka, thus entrenching the divide between the depression and the valley. Gross correlations with Pleistocene deposits of the Nile Valley and the Kharga Depression are based upon archeological evidence only until more precise geochronology can be applied to the problem.*

Between the desert spring of Dungul at the south end of the Eocene plateau of Egypt and Bir Kiseiba, 200 km to the west-southwest, there is an irregularly shaped, internally drained basin about 17,000 km^2 in area that lies at an elevation below 180 m (Fig. 1). This area, which I shall call the Kiseiba-Dungul Depression, has been described as a pediplain (*1*, *2*) and is separated from the Nile Valley by a broad sandstone ridge with high points between 200 and 300 m. Thirty-four kilometers northeast of the restored temples at Abu Simbel a dry stream bed called Wadi Tushka heads on the divide between the Kiseiba-Dungul Depression and the Nile Valley. Close to the divide, the wadi becomes inconspicuous. A number of long-inactive mud pans (playas) at an elevation between 174 and 180 m extend farther northwestward across the inconspicuous divide.

The Aswan High Dam can retain Lake Nasser at a maximum level of 183 m, but, by excavating a spillway along the axis of Wadi Tushka, the High Dam Authority plans to be able to divert excess water from any rise above 178 m to the Kiseiba-Dungul Depression for irrigation agriculture. Thus the Sadat Canal project can be an effective means of conserving irreplaceable groundwater if care is taken to avoid the accumulation of salt in an environment where evaporation rates (*3*) are among the highest known.

More than 50 years ago John Ball asked whether the Nile, or a branch of it, ever flowed through the Libyan Desert to the Mediterranean. After reviewing

0036-8075/80/1003-0068$00.50/0